Indonesian Journal of Electrical Engineering and Computer Science
Vol. 29, No. 2, February 2023, pp. 1174~1182
ISSN: 2502-4752, DOI: 10.11591/ijeecs.v29.i2.pp1174-1182

Automatic recognition of color sensation with controlled phosphene brightness using pre-trained CNNs framework

Muthyala Veera Venkata Satyanarayana Chowdary, Teppala Venkata Ramana
Department of EECE, GITAM Deemed to be University, Visakhapatnam, India

Article Info

Article history:

Received Jul 22, 2022
Revised Sep 22, 2022
Accepted Oct 24, 2022

Keywords:

Argus-II dataset
Automatic adjustment of electrical stimuli
Correlation based feature selection
Pre-trained CNNs

ABSTRACT

Argus-II is one of the most successful epiretinal implantation for providing visual acuity those who lost their vision sight due to retinitis pigmentosa (RP) problem. However, this model faces color recognition issue is observed from implanted patients. Hence, it arises whenever electrode fail to retain same electrical stimuli property during sensitivity color transition state is occurred (especially, blue and purple colors). To resolve this problem, a proper handling of electrical stimuli parameters (amplitude, frequency and pulse width) is required during patient under every visual impact is possible. Addition to this, the individual patient color sensation is recorded in the observation state and creates Argus-II dataset to train the machine learning algorithm for maintaining phosphene brightness through controlled generation of the electrical stimuli. Therefore, in this paper, an automatic recognition of color sensation with controlled phosphene brightness using pre-trained convolutional neural network (CNNs) framework is proposed. The frequency modulated electrical stimulation of retina is purely influence by trained CNNs for adjusting amplitude that can retain maximum brightness along with clarity in the color sensation. The experimental results shows that the proposed system is achieved reasonable improvement in the transition color sensation as well as controlled brightness when compared with other existing systems.

Corresponding Author:

Muthyala Veera Venkata Satyanarayana Chowdary
Department of EECE, GITAM Deemed to be University
Gandhi Nagar, Rushikonda, Visakhapatnam, Andhra Pradesh 530045, India
Email: mvvsvenkatchowdary716@gmail.com

1. INTRODUCTION

Human eye is always has a significant quality of sensing multi-colors on the image undergoes several levels of visual processing [1]. Color aids in the segmentation of the visual scene and increases the saliency of visual inputs at lower and higher levels, items viewed in their characteristic colors are linked to color knowledge stored in memory [2]–[4]. Color vision is initiated from cone photoreceptors (S, M, and L) which are highly sensitive to light wavelength including all ranges (short, medium, and long) respectively. It is commonly accepted that color vision encoding is translated from these three types of cones to three separate opponent systems early in the visual pathway: red (R), green (G), blue (B), yellow (Y), and black-white [5], [6]. Around 30 to 50 million people suffered by the retinal degeneration which is a major root cause of blindness globally [7]. Normally, outer layer of the photoreceptors are completely fade-out at the end stage. As results, patients deprive their capacity to perceive light and color [8], [9]. Surgical retinal implantation can help restore vision by stimulating the remaining inner retinal neurons. However, it follows under lower spatial resolution of 16 to 1600 electrodes [10]–[13]. As a result, any method of increasing visual information for object recognition and orientation in a given context is beneficial [14]. However, such an approach for providing limited color feeling as an additional dimension of vision in retinal prosthetics. Argus-II is one of the most successful epiretinal implantations for restoring eyesight to people who have lost their vision due to retinitis pigmentosa (RP). However, implanted individuals have reported that this model has a color recognition problem [15]. As a result, it occurs when an electrode fails to maintain the same electrical stimulation property during the sensitivity color transition stage [16]–[18]. To tackle this difficulty, adequate handling of electrical stimulation characteristics (amplitude, frequency, and pulse width) is essential during the patient's treatment under all conceivable visual impacts. Furthermore, during the observation stage, each patient's color experience is recorded, resulting in the creation of the Argus-II dataset, which is used to train the machine learning algorithm for sustaining phosphene brightness through controlled generation of electrical stimuli. As a result, utilizing a pre-trained convolutional neural network (CNNs) framework, an automatic recognition of color feeling with controlled phosphene brightness is proposed in this research. The amplitude of frequency modulated electrical stimulation of the retina is only influenced by trained CNNs for retaining maximum brightness and clarity in the color sense. When compared to other current systems, the experimental findings reveal that the suggested system achieves a reasonable improvement in transition color sense as well as controlled brightness [19].

The organization of paper is given as follows: Section 2 describes overview of the methodology and elaborates about Argus-II datasets. Section 3, discuss the experimental results includes electrical stimuli adjustment with controlled phosphene brightness, Color sensation changes as a function of stimulated frequency, maintain Long-term stability towards color sensation and correlation-based feature extraction algorithm. Finally, conclusion and future scope is given in section 6.

2. MATERIALS AND METHOD

2.1. Argus-II dataset

In this paper, mainly focusing on enhance the accurate color restoring process is initiated automatically by using pre-trained CNNs framework. The Argus-II is well-known surgical implantation is developed to activate ganglion cell which is not affected by retinitis pigmentosa (RP) problem. It consists of linear array (6x10) of electrodes are arranged to receive electrical stimuli with respect to visual scenes. This set up is placed on both eye of the patient who has affected by RP degradation. In [13] described the experimental study to understand the visuality functioning of the Argus-II on implanted patient. Nearly, 7 interested members (5 female and 2 males) are participated in the testing phase in which daily observation details are recorded for further analysis is carried in future (if required). Additionally, different time stamp of Argus-II surgical implanted patients are subjected in the study (i.e. years between 2015 and 2019) and patients are registered that they have clear vision in their childhood days due to age factor vision perception quality is affected which leads into loss of sight. The training features are derived from patient recorded which is applied to CNNs for obtaining trained datasets for better color sensation with controlled phosphene brightness is achieved [20]. That implies, amount of current passing to each electrode is automatically adjusted based on the trained dataset receive from pre-trained CNNs framework [21]–[23]. Usually, the feature extraction of current level thresholding is obtained based on patient records observed during the Argus-II test phase. That means, patients are advice to give response (‘yes’ or ‘no’) according to their perceived phosphene quality and respective electrical stimulus is recorded. They are given six different options to register their response (i.e. not detected, dim, dim to medium, medium, medium to bright and bright). Internally, several threshold points are generated and process can be optimized after desired target current level is reached. The individual electrode current level ($I_{electrode} \approx 168\mu A$) is identified for an automatic recognition of color sensation with controlled phosphene brightness [24]. The artificial intelligence (AI) algorithm is programmed to initiate automatic formation electrodes in groups (either pairs or quads) based on current level threshold. Thereby, if $I_{electrode}$ is greater than $I_{electrode\_threshold}$ then, group formation is restricted. Otherwise, it allows for electrode group formation$\left(I_{electrode_threshold} \leq I_{electrode}\right)$. Because of group formation, minimize the chance of tissues damage due to lower value selection of the electrode current. The AI algorithm is more effective to adjust electrode current $I_{electrode}$may arias fluctuations and maintains identical electrical stimuli for entire electrode group [25].

2.2. Color categories model

The patients are subjected to understand the color transition state by giving suitable example that describes color sensation by classifying into two set namely hue (color detection is wrong due to much similarity color shade is observed by patient) and saturation (color detection is wrong due to unawareness about the color scaling bands is exhibited by patient). According to the patient response, brightness is adjusted manually from external system during testing phase. The RYGB color model is adapted for recognizing color shades (eg: pink, red, brown and green). All colors can be labeled using different proportions of fundamental hue perceptions in red (R), yellow (Y), green (G), and blue (B) in this model [18]. In general, color shades of blue and yellow are normalized to achieve quality color sensation with controlled phosphene brightness. It is denoted by vector sets such as $S_1 = (b_1, b_2, \ldots. b_n)$ and $S_2 = (y_1, y_2, \ldots. y_m)$where, $n$and $m$be the maximum color shades present in the blue and yellow. Because, patient may faces difficulty to differentiate blue and yellow shade colors respectively. Even, amount of hue and saturation perception are unable to predict the accurate color classification. The saturation scaling range lies between minimum and maximum point (i.e.$\gamma = (0.2 - 0.5)$). Especially, royal purple, lavender purple, royal yellow and lemon yellow comes under blue and yellow color shade. All other colors are classified correctly by the patient.

2.3. Blue and Yellow score calculation

The blue score is not differentiated between blue and purple because the observed purple colors are highly blue biased, and the current study is focused on the yellow-blue color pathway. The data were analysed using paired sample t tests. It was done in R with a significance level of 0.05. Curve fits were improved and weighted with the inverse of variance. The following pseudo code is representing scaling system used in the color categories model to calculate a blue and yellow score for each color sensation is given below:

AI algorithm for blue and yellow scoring

#1 *Initialization:* $I_{electrode} = 168\mu A$, $S_1 = (b_1, b_2, \ldots. b_n)$and $S_2 = (y_1, y_2, \ldots. y_m)$
#2 *Saturation scaling:* 0.2 to 0.5
#3 **for** i=1 to No of patients
#4 Identify brightness of individual patient and compute $I_{electrode}$
#5 **If** $I_{electrode} \leq 168$, then
#6 **Set** electrode group formation and maintain identical electrical stimuli
#7 **else** $I_{electrode} > 168$then,
#8 **Set** restrict the group formation
#9 **Update** optimized $I_{electrode}$from individual patient response
#10 **Update** feature training dataset
#11 **If** $\gamma \leq 0.2$then,
#12 **Set** $S_1 = S_2 = 1$; blue (S_1)/yellow (S_2)sensation, the hue is unsaturated.
#13 **else if** $\gamma = 0.2\&\&0.5$then,
#14 **Set** $S_1 = S_2 = 2$; blue (S_1)/yellow (S_2)sensation, hue is significantly reported.
#15 **else if** $\gamma > 0.5$then,
#16 **Set** $S_1 = S_2 = 3$; blue (S_1)/yellow (S_2)sensation, strongly reported.
#17 **else** $\gamma = 0$then,
#18 **Set** $S_1 = S_2 = 0$; No perception

3. MATERIALS AND METHODOLOGY

In this part, the qualitative analysis of the suggested model is carried out by various stimulation frequencies to address an automated adjustment of electrical stimuli for improving brightness, ensuring proper colour recognition. Pre-trained CNNs update feature extraction sets to generate quality training samples from Argus-II patient database. It has 7 members (5 females and 2 males) who record daily observations for analysis (if required). The proposed approach uses pre-trained CNNs to improve automated colour restoration. Experimental validation is performed by varying stimulation settings such as frequency from 6 to 120 Hz and pulse width from 0.2 to 2 ms. In this research, Argus-II has 29 electrodes implanted and recognises 11 colours: grey, white, yellow, dark yellow, purple, gold, green, blue, pink, black, orange, and brown. 3 of 11 hues (grey, black, and white) are chromatic, while 8 are not.

3.1. Electrical stimuli adjustment with controlled phosphene brightness

Patient data show that inadequate electrode current causes colour sense problems. Monitoring patient reaction and adjusting electoral stimuli helps decrease colour sensory problems. Figure 1 shows patients' responses to modulate phosphene brightnes observed by prosthetic eyesight. For experimental consideration we used Indian street side purple flower plants taken for color sensation analysis whose indivudal resolution is clearly mentioned as (a) 273x 376 pixels, (b) 27x36 pixels, (c) 3x6 pixels, (d) 573x 400 pixels, (e) 64x32 pixels and (f) 9x3 pixels respectively. Figure 2 depicts the color sensation response obtained from patients with controlled phosphene brightness. According to Argus-II patient response data, two types of colour sensory abnormalities are identified: yellow to blue and blue to purple. Figure 2(a) and Figure 2(b) show the stimulated pulse wave and current amplitude for medium brightness. Pre-trained CNNs improve electrical stimulation by changing electrodes depending on feature sets. Figure 2 (c) shows dominant hues and needed electrodes for each. Chromatic colours need more than 5 electrodes, whereas other colours require less. Purple and yellow are other popular colours. Figure 2 shows blue-yellow and red-green axes (d). Color and size of circles indicate perceived colour and fundamental frequency.

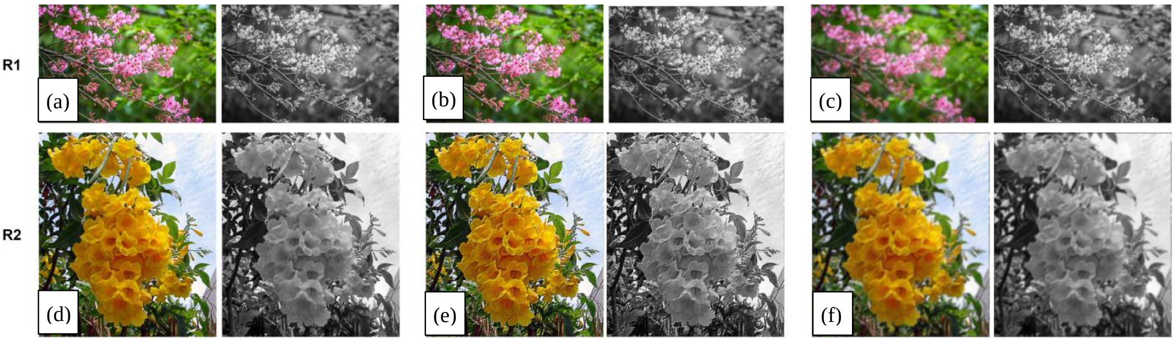

Figure 1. The importance of simulated prosthetic eyesight is demonstrated. R1: Colored and greyscale represents Indian street side purple flower plants consider for color sensation analysis (a) 273x 376 pixels, (b) 27x36 pixels, (c) 3x6 pixels. R2: Colored and greyscale represents Indian street side yellow flower plants consider for color sensation analysis (d) 573x 400 pixels, (e) 64x32 pixels, and (f) 9x3 pixels respectively

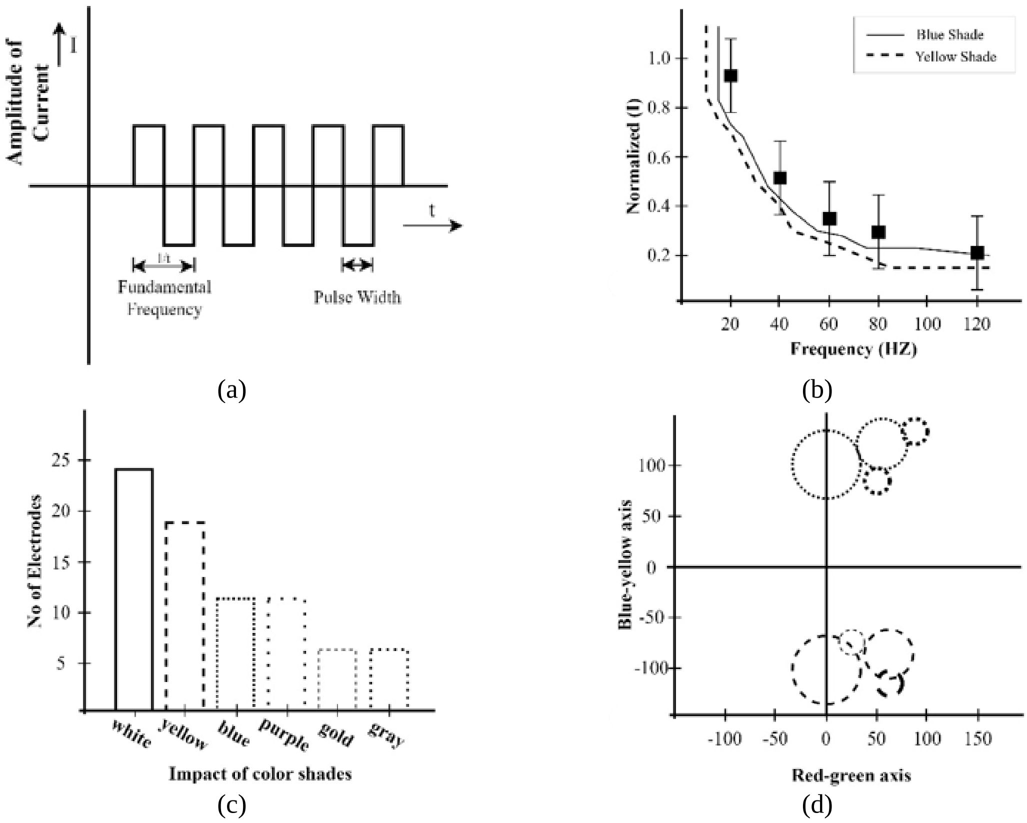

Figure 2. Color sensation response obtained from patients with controlled phosphene brightness. (a) waveform indicates stimulated pulse at medium brightness with frequency modulation; (b) current amplitude required to keep medium brightness (Im) as frequency increases (Results observed from 29 electrodes and recorded patient's responses that converge exponentially towards target point, where 'R' is equal to 0.94); (c) colors dominant and number of electrodes generating each color are represented (chromatic colors are required more than 5 electrodes for identification, others colors identify by less than 5 electrodes which is not shown) and (d) color space generated by blue-yellow and red-green axis, where purple and yellow color shades are often undergo color sensation. The circles' color and size represent the perceived color and its fundamental frequency, respectively

3.2. Color sensation changes as a function of stimulated frequency

Changing the current amplitude may change the colour sense. In this part, patient responds to varied frequency (50, 100, 150) and pulse width (0.5, 1, 1.5 and 2 ms). Figure 3 depicts it, when the stimulated frequency shifts from low (less than 60 Hz) to high (greater than 60 Hz), implanted individuals see a yellow-to-blue transition. In Figure 3(a), colour perception shifts from yellow to blue when stimulus frequency is between a few Hz and 150 Hz. If many colours are identified in one phosphene, they are represented in concentric circles, each signifying hue and saturation. Figure 3(b) shows the colour sensory response of three female and one male patients implanted two years ago. Their perception changed from yellow (less than 60 Hz) to white (more than 60 Hz) when stimulation frequency varied between a few Hz and 150 Hz. Color perception is high by using more electrodes to create true colour bands, even if they are between two colours. Figure 3(c) shows colour perception from 8 electrodes in distinct retinal areas with frequency fluctuations (PW=0.5). Purple and yellow are colour sensations. It is noticed from blue-yellow and red-green axes independently under frequency changes Figure 3(d). It doesn't change much between 0 and 1.2 pulse width.

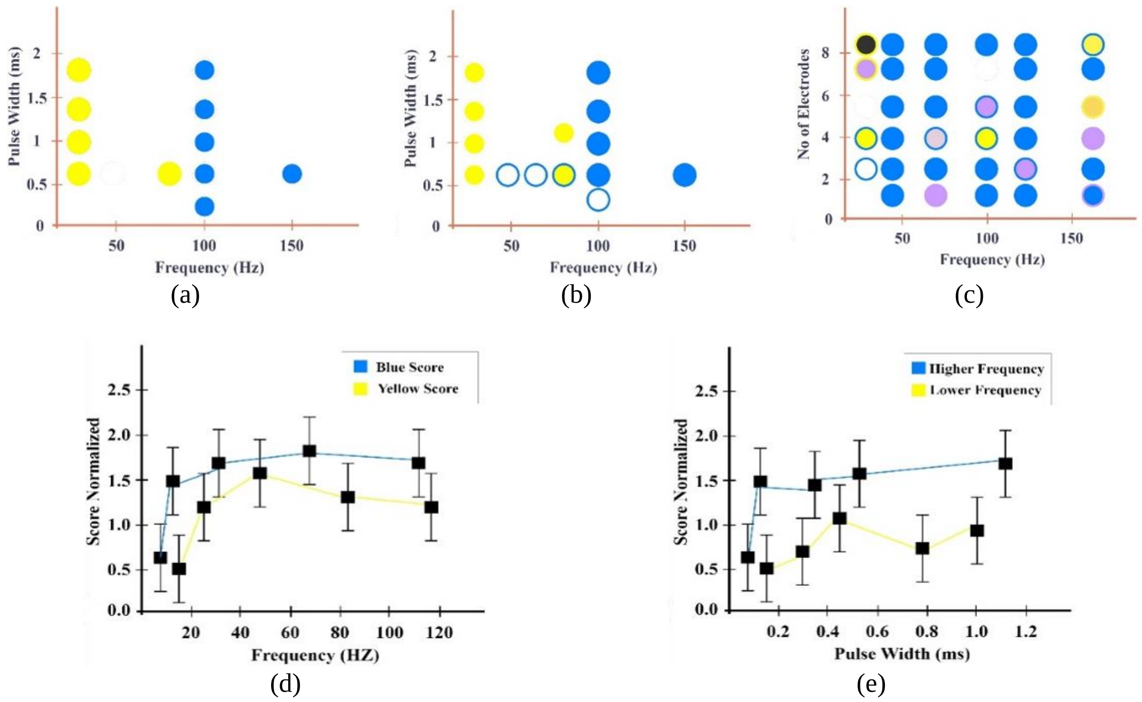

Figure 3. Illiterate the influence of stimulus frequency and pulse width (PW) on color perception. For experimental validation follows different combination of the stimulated frequency (50, 100, and 150) and pulse width (0.5, 1, 1.5, and 2 ms). (a) results examine that the subjected patients (2 female and 1 male) who got recent implantation, they have perception changed from yellow (less than 60 Hz) to blue (greater than 60 Hz), when stimulation frequency changes in the range between a few Hz and 150 Hz. If more than one color has detected in one phosphene, they are shown in concentric rings, each representing the hue and saturation of one color; (b) results examine that the subjected patients (3 female and 1 males) implanted two years ago for them perception changed from yellow (less than 60 Hz) to white (greater than 60 Hz), when stimulation frequency changes in the range between a few Hz and 150 Hz; (c) color perception from 8 electrodes in various retinal regions of both type of implantation (recent and two years old) with frequency variations (PW=0.5); (d) aggregated blue and yellow scores under frequency variations, and (e) Aggregated blue and yellow scores under pulse width varying between 0 and 1.2 respectively

3.3. Electrically adjusted and maintain Long-term stability towards color sensation

Figure 4 indicates high-frequency purple enhances colour perception. Color as a dependable dimension of visual cues in prosthetic vision depends on the long-term stability of the electrically evoked color experience. As a result, compared the color perception of two type of patient based on period of implantation such as (i) patient of (5 months < implanted year < 10 months) and (19 months < implanted year < 30 months) who were subjected for analysis under different frequencies. Pooling blue and purple data. Recent implants may cause color-sensation issues, particularly at low and high frequencies. Argus-database II indicates that colour perception is independent of patient health and age, therefore automatic stimulus adjustment preserves medium brightness. Pre-trained CNNs employ correlation-based feature extraction to differentiate colour index profiles like royal yellow, lemon yellow, royal purple, lavender purple. Figure 4(a) shows the implanted patient's frequency-dependent colour perception. Similar yellow colour index colours become indistinguishable after a few months. Electrodes don't obtain a steady current, therefore electrical stimulation is distributed, impairing the implanted patient's brightness. Figure 4(b) shows the implanted patient's frequency-dependent colour perception. People can't tell purple from blue after a few years. These two problems may be overcome by restoring current amplitude using updated CNN feature sets. In Figure 4(c), pre-trained CNNs enhance colour perception by minimising low-to-high frequency yellow-to-blue transitions (recent implanted patient). Low frequency yellow colour shades are artificial, however implanted patients can't detect true colour (yellow index) due to lack of brightness. Pre-trained CNNs recognise electrodes that need current amplitude adjustment and operate them with a constant quantity of current to ensure medium brightness for categorising related colour index issues. Figure 4(d) shows the maximum number of electrodes that can correctly modify electrical stimuli, yellow for low frequency. Proper electrode selection (target of 5 electrodes) is needed to modify electrical stimuli based on CNN feature sets. Figure 4(e) and Figure 4(f) illustrates the number of yellow-to-blue and blue-to-purple electrodes.

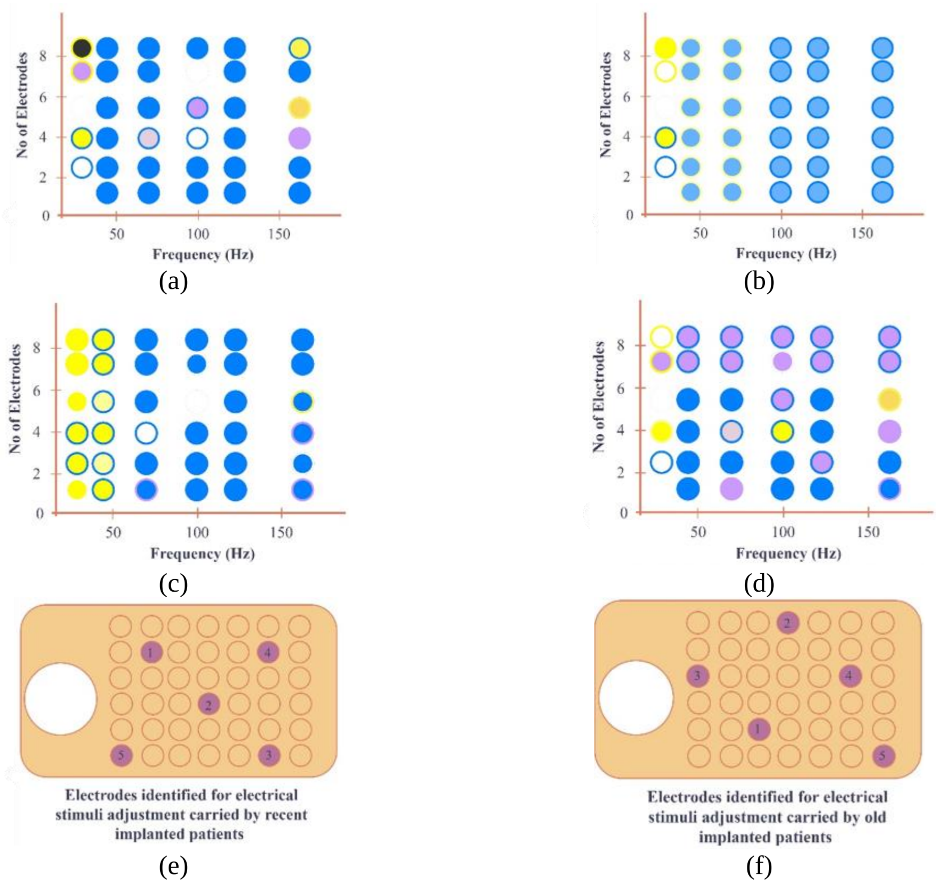

Figure 4. Response of color sensation (yellow to blue and blue to purple) tracked from recent and two-year-old implanted patient under frequency-shifting over time. (a) color perception response of the recent implanted patient (5 months < implanted year < 10 months) under different frequencies; (b) color perception response of the old implanted patient (19 months < implanted year < 30 months) under different frequencies; (c) enhanced color perception using pre-trained CNNs which minimize color sensation problem of yellow to blue transition phase at varying frequencies from low to high (recent implanted patient); (d) enhanced color perception using pre-trained CNNs which minimize color sensation problem of blue to purple transition phase at varying frequencies from low to high (old implanted patient). Electrodes (target no of electrodes 5) identified for adjusting electrical stimuli based on feature sets updated by pre-trained CNNs and (e) for yellow to blue, and (f) for blue to purple sensation respectively

3.4. Correlation based feature extraction algorithm

After image segmentation, feature extraction is crucial. It captures quiet characteristics from each unit for subsequent analysis to uncover segmented process irregularities. It uses grey level intensity to quantify statistical parameters. It helps identify colour index and pattern observation problems. Figure 5 exhibits correlation-based feature extraction in pre-trained CNNs. Second order statistical parameters are used to generate the textural feature set based on the grey level intensity (minimum 14) of each pixel and its neighbouring pixels. Two-dimensional matrix is used to analyse image spatial property by adjusting pixel intensity based on occupied frequencies. First, a pixel to the right of the reference pixel may vary its intensity between minimum and maximum threshold limits (i.e. 2 to 256). It also gives favourable and unfavourable criteria to assist attain minimal membership function quicker and pass the first phase of optimization. Because it involves entropy and contrast, it shows high and low pixel intensities. Here's how the training and test phase works.

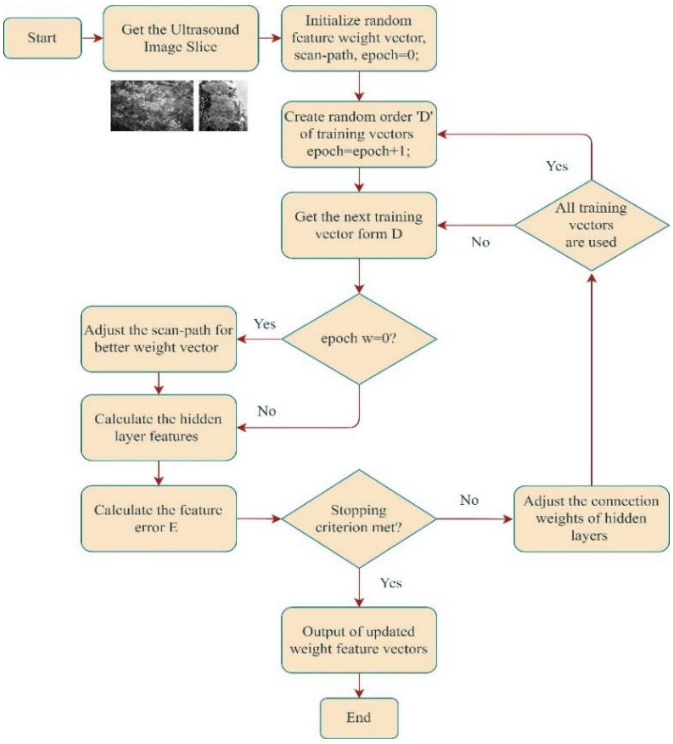

Figure 5. Operational flow of correlation-based feature extraction approach involved in the pre-trained CNNs

a. Training phase:
   - Initializing the number of iterations is carried out for finding weight vector and euclidean distance for effective feature selection. Approximately, set the cluster group size is equal to 30 or it will be adjusted to convergence range.
   - Clustering feature sets are extracted in the training phase for identifying extract feature mapping with ground truth images. By using equation of $I_{electrode}$ and γ as mentioned in the pseudo code are updating regularly based on the instant weight vector of each frame.
   - Similarly, it has continued for all other data sets in order to estimate the cost function as closer to desired target based on the favourable and unfavourable criterion derived from pre-trained CNN extraction model.
   - Once the cost function is converged, then it is fixed for selecting best threshold value by setting local and global factor using correlated based feature selection algorithms.

b. Testing phase:
   - Testing phase is activated if the pre-trained CNN parameters are not converge then further updating is carried in the weight vector for withstanding best threshold value. Every sample output is recorded, and it is being validated after entire sample undergoes double optimization process. Figure 6 and Figure 7 show the normalised scores of the chosen electrodes (5) for higher responsiveness under blue to purple feeling (recently implanted patient) (old-implanted patient). Pre-trained CNN architecture gives enough brightness to classify colour tones. Figure 6 and Figure 7 show TPR and FPR improvement and maintained trade-off ratio.

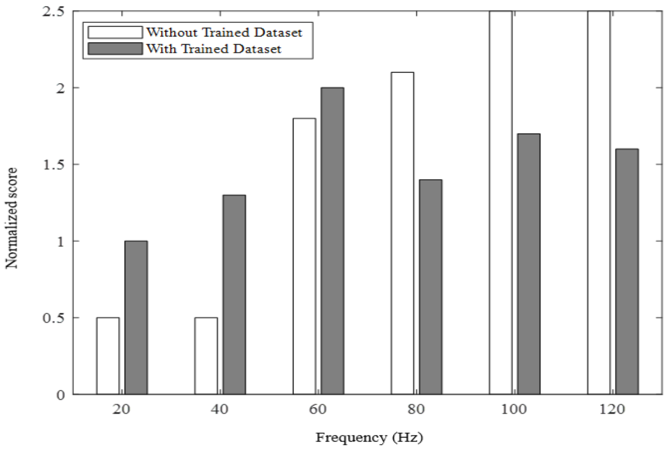

Figure 6. Normalized scores of the targeted electrodes (5 in numbers) for better response under yellow to blue sensation state recorded (recent implanted patient)

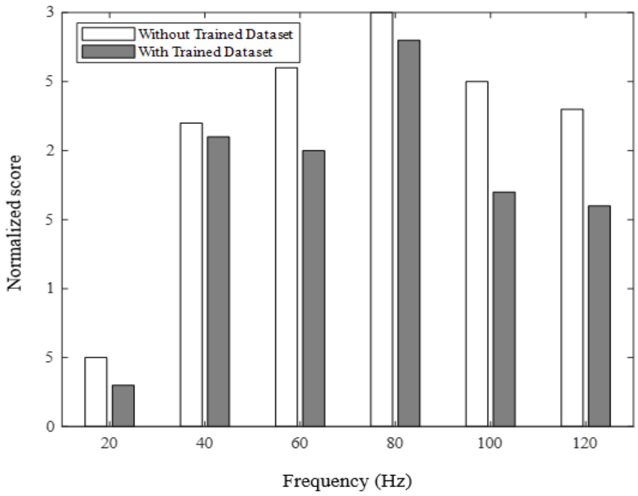

Figure 7. Normalized scores of the targeted electrodes (5 in numbers) for better response under blue to purple sensation state recorded (old-implanted patient)

4. CONCLUSION

In this paper, an automatic recognition of color sensation with controlled phosphene brightness using pre-trained CNNs framework is proposed. The training features are derived from patient recorded which is applied to CNNs for obtaining trained datasets for better color sensation with controlled phosphene brightness is achieved. That implies, amount of current passing to each electrode is automatically adjusted based on the trained dataset receive from pre-trained CNNs framework. The feature extraction of current level thresholding is obtained based on patient records observed during the Argus-II test phase. Thereby, pre-trained CNNs provides updated feature set in order to detect the accurate electrodes who need current amplitude adjustment is effectively identified and operate those electrodes with standard amount of current which ensure medium brightness for classifying similar color index problem. The experimental results shows that the proposed system is achieved reasonable improvement in the transition color sensation as well as controlled brightness when compared with other existing systems.

REFERENCES

[1] I. Bramão, A. Reis, K. M. Petersson, and L. Faísca, "The role of color information on object recognition: A review and meta-analysis," *Acta Psychol. (Amst).*, vol. 138, no. 1, pp. 244–253, Sep. 2011, doi: 10.1016/j.actpsy.2011.06.010.
[2] J. Tanaka, D. Weiskopf, and P. Williams, "The role of color in high-level vision," *Trends Cogn. Sci.*, vol. 5, no. 5, pp. 211–215, May 2001, doi: 10.1016/S1364-6613(00)01626-0.
[3] B. Rossion and G. Pourtois, "Revisiting snodgrass and vanderwart's object pictorial set: the role of surface detail in basic-level object recognition," *Perception*, vol. 33, no. 2, pp. 217–236, Feb. 2004, doi: 10.1068/p5117.

[4] B. Uttl, P. Graf, and P. Santacruz, "Object color affects identification and repetition priming," *Scand. J. Psychol.*, vol. 47, no. 5, pp. 313–325, Oct. 2006, doi: 10.1111/j.1467-9450.2006.00532.x.

[5] J. Nathans, "The evolution and physiology of human color vision: insights from molecular genetic studies of visual pigments," *Neuron*, vol. 24, no. 2, pp. 299–312, Oct. 1999, doi: 10.1016/S0896-6273(00)80845-4.

[6] D. M. Dacey, "Circuitry for color coding in the primate retina.," *Proc. Natl. Acad. Sci.*, vol. 93, no. 2, pp. 582–588, Jan. 1996, doi: 10.1073/pnas.93.2.582.

[7] N. M. Bressler, "Age-related macular degeneration is the leading cause of blindness . . .," *JAMA*, vol. 291, no. 15, p. 1900, Apr. 2004, doi: 10.1001/jama.291.15.1900.

[8] A. I. D. Hollander *et al.*, "Mutations in a human homologue of drosophila crumbs cause retinitis pigmentosa (RP12)," *Nat. Genet.*, vol. 23, no. 2, pp. 217–221, Oct. 1999, doi: 10.1038/13848.

[9] G. R. Jackson, C. Owsley, and C. A. Curcio, "Photoreceptor degeneration and dysfunction in aging and age-related maculopathy," *Ageing Res. Rev.*, vol. 1, no. 3, pp. 381–396, Jun. 2002, doi: 10.1016/S1568-1637(02)00007-7.

[10] D. T. Hartong, E. L. Berson, and T. P. Dryja, "Retinitis pigmentosa," *Lancet*, vol. 368, no. 9549, pp. 1795–1809, Nov. 2006, doi: 10.1016/S0140-6736(06)69740-7.

[11] P. E. Stanga *et al.*, "Argus II electronic epiretinal prosthesis in advanced dry AMD: safety and feasibility study and preliminary functional results," *ARVO Annu. Meet. Abstr.*, vol. 58, no. 8, 2017.

[12] K. Stingl *et al.*, "Subretinal visual implant alpha IMS – clinical trial interim report," *Vision Res.*, vol. 111, pp. 149–160, Jun. 2015, doi: 10.1016/j.visres.2015.03.001.

[13] L. Yue, J. D. Weiland, B. Roska, and M. S. Humayun, "Retinal stimulation strategies to restore vision: Fundamentals and systems," *Prog. Retin. Eye Res.*, vol. 53, pp. 21–47, Jul. 2016, doi: 10.1016/j.preteyeres.2016.05.002.

[14] P. E. Stanga *et al.*, "Patients blinded by outer retinal dystrophies are able to perceive color using the Argustm ii retinal prosthesis system," *Invest. Ophthalmol. Vis. Sci.*, vol. 52, no. 14, p. 4949, 2011.

[15] R. Hornig, T. Zehnder, M. Velikay-Parel, T. Laube, M. Feucht, and G. Richard, "The IMI retinal implant system," in *Artificial Sight*, New York, NY: Springer New York, 2007, pp. 111–128. doi: 10.1007/978-0-387-49331-2_6.

[16] P. E. Stanga *et al.*, "Patients blinded by outer retinal dystrophies are able to perceive simultaneous colors using the Argus® II retinal prosthesis system," *ARVO Annual Meeting Abstract*, vol. 53, no. 14, 2012, [Online]. Available: https://iovs.arvojournals.org/article.aspx?articleid=2360651

[17] A. E. Hadjinicolaou *et al.*, "Optimizing the electrical stimulation of retinal ganglion cells," *IEEE Trans. Neural Syst. Rehabil. Eng.*, vol. 23, no. 2, pp. 169–178, Mar. 2015, doi: 10.1109/TNSRE.2014.2361900.

[18] H. C. Stronks and G. Dagnelie, "The functional performance of the Argus II retinal prosthesis," *Expert Rev. Med. Devices*, vol. 11, no. 1, pp. 23–30, Jan. 2014, doi: 10.1586/17434440.2014.862494.

[19] J. Gordon, I. Abramov, and H. Chan, "Describing color appearance: hue and saturation scaling," *Percept. Psychophys.*, vol. 56, no. 1, pp. 27–41, Jan. 1994, doi: 10.3758/BF03211688.

[20] T. M, V. R, G. M, R. M, M. P, and N. S, "Efficient classification of heart disease using KMeans clustering algorithm," *Int. J. Eng. Trends Technol.*, vol. 68, no. 12, pp. 48–53, Dec. 2020, doi: 10.14445/22315381/IJETT-V68I12P209.

[21] P. Vasudevan and T. Murugesan, "Cancer subtype discovery using prognosis-enhanced neural network classifier in multigenomic data," *Technol. Cancer Res. Treat.*, vol. 17, p. 153303381879050, Jan. 2018, doi: 10.1177/1533033818790509.

[22] B. Kalaiselvi and M. Thangamani, "An efficient pearson correlation based improved random forest classification for protein structure prediction techniques," *Measurement*, vol. 162, p. 107885, Oct. 2020, doi: 10.1016/j.measurement.2020.107885.

[23] S. Ramesh and T. R. Rao, "Indoor channel characterization studies for V-band gigabit wireless communications using dielectric-loaded exponentially tapered slot antenna," *Int. J. Microw. Wirel. Technol.*, vol. 8, no. 8, pp. 1243–1251, Dec. 2016, doi: 10.1017/S1759078715000781.

[24] S. Markkandan, S. Sivasubramanian, J. Mulerikkal, N. Shaik, B. Jackson, and L. Naryanan, "Massive MIMO codebook design using gaussian mixture model based clustering," *Intell. Autom. Soft Comput.*, vol. 32, no. 1, pp. 361–375, 2022, doi: 10.32604/iasc.2022.021779.

[25] P. E. Stanga *et al.*, "Argus II electronic epiretinal prosthesis in advanced dry AMD: safety and feasibility study and preliminary functional results," *ARVO Annu. Meet. Abstr.*, vol. 58, no. 8, 2017.

BIOGRAPHIES OF AUTHORS

Muthyala Veera Venkata Satyanarayana Chowdary he is a research Scholar in the Department of Electronics and Communications Engineering, GITAM Deemed to be University Visakhapatnam, received B.Tech degree in Electronics and Communications Engineering from JNTU Kakinada in 2012, M.Tech degree in VLSI SYSTEM DESIGN from JNTU Kakinada in 2016. His research areas are Image Video processing, VLSI and Artificial Intelligence. His research topics are published in several National International Journals. He can be contacted at email: mvvsvenkatchowdary716@gmail.com.

Dr. Teppala Venkata Ramana as a diligent scholar, has obtained his Bachelor's Degree in Electronics Communications Engineering from Nagarjuna University in the 1989, Masters in Systems and Control Engineering from Osmania university in the year 1998 and completed Doctoral program Ph.D. in the area of Satellite Communications from the Andhra University in the year 2012, conducted a number of conferences, workshops for an academic excellence. He has guided a big number of technical projects and also directing a number of scholars (12) towards their doctoral program (PhD). He has more than 35 publications on an assortment of topics in reputed national international journals and conferences and the Life member of IETE ISTE, and fellow of ISRD. He can be contacted at email: vteppala@gitam.edu.